Composites Science and Technology 190 (2020) 108043

Contents lists available at ScienceDirect

Composites Science and Technology

journal homepage: http://www.elsevier.com/locate/compscitech

High-performance and functional PBT/EVMG/CNTs nanocomposites from recycled sources by in situ multistep reaction-induced interfacial control

Ying Cao [a], Pengwu Xu [a,b], Baogou Wu [a], Martin Hoch [c], Pieter Jan Lemstra [d], Weijun Yang [a], Weifu Dong [a], Mingliang Du [a], Tianxi Liu [a], Piming Ma [a,*]

[a] The Key Laboratory of Synthetic and Biological Colloids, Ministry of Education, Jiangnan University, 1800 Lihu Road, Wuxi, 214122, China
[b] Institute of Physics, University of Freiburg, Hermann-Herder-Street 3, 79104, Freiburg, Germany
[c] ARLANXEO High Performance Elastomers (Changzhou) Co. Ltd, Shanghai Branch, South Huangpi Road, Shanghai, 200025, China
[d] PlemPolco B. V., De Zicht 11, 5502 HV, Veldhoven, the Netherlands

ARTICLE INFO

Keywords:
Poly (butylene terephthalate)
Super-tough
Conductivity
Rheological modification

ABSTRACT

Super-tough and antistatic poly (butylene terephthalate) (PBT) composites from recycled sources with carbon nanotubes were prepared by a multistep reactive compounding process. The PBT-modification was accomplished using epoxidized elastomers (EVMG), epoxidized multi-walled carbon nanotubes (e-CNTs) and epoxidized rheology modifiers (ADR). The reaction between epoxy and PBT-COOH (or –OH) groups enhanced the interfacial bonding between the PBT matrix and the dispersed EVMG and CNTs phases. Moreover, the distribution of CNTs is exclusively in the PBT phase. The presence of ADR resulted in a larger viscosity ratio of the PBT phase to the EVMG phase due to the PBT chain extension and branching, which led to a smaller EVMG particle size and a shorter inter-particle distance. Consequently, both the mechanical properties and the electrical conductivity of the PBT composites were considerably improved due to a synergistic effect of the EVMG and the ADR, e.g., the notched impact strength of the PBT composites reached up to 88 kJ/m^2 and the percolation threshold value for conductive network was reduced by 27%. The super-tough and antistatic PBT composites designed in this study may broaden the application range of PBT in automotive and electrical applications.

1. Introduction

Poly (butylene terephthalate), PBT, as one of the engineering plastics, is widely applied in electrical applications, automotive parts, machinery and also some other fields due to its solvent resistance, high strength, fatigue resistance, processing stability etc [1,2]. However, PBT is a typical notch-sensitive material with poor impact strength of approximately 4 kJ/m^2 [2–4], which is one of the major obstacles for its application in automotive electrical areas. Another disadvantage is the accumulation of electrical charges on the surface of PBT articles and these articles will release static electricity especially in dry environment, which might be harmful to the human body and electrical equipment [5]. Therefore, it is important to simultaneously increase the toughness and conductivity to broaden the application range of PBT materials.

Many routes have been explored to toughen PBT such as copolymerization [6–8], plasticization [9], chain extension [10] and blending [11–13], in which blending with elastomers is an effective and economic method for initiating brittle-to-ductile transition. In the presence of external forces, elastomer particles in PBT/elastomer blends may cause a large amount of crazing and/or shear bands in the matrix, which can absorb ample energy and prevent crack propagation, thereby exerting a toughening effect. Meng et al. [13] increased the notched impact strength of PBT to 8 kJ/m^2 by compounding PBT with ethylene-vinyl acetate copolymer (EVA) where the EVA particle size is nearly 6.5 μm. Yang et al. [14] blended PBT with polyolefin elastomer using ethylene-butylacrylate-glycidyl methacrylate (PTW) as a reactive compatibilizer which reduced the particle size of elastomer from 3.0 to 0.8 μm. Consequently, the notched impact strength of PBT increased from 5 to 50 kJ/m^2 while the tensile strength remained at 30 MPa. These studies have shown that a uniform dispersion of elastomer particles and a strong interfacial bonding between the dispersed elastomer particles and the PBT matrix are essential for property improvement.

PBT can be made antistatic or even conductive by incorporating conductive fillers such as carbon black [15], multi-walled carbon nanotubes (MWCNTs) [16,17] or graphene [18,19], and this modified PBT can be used as an antistatic and electromagnetic shielding material.

* Corresponding author.
E-mail address: p.ma@jiangnan.edu.cn (P. Ma).

https://doi.org/10.1016/j.compscitech.2020.108043
Received 13 November 2019; Received in revised form 18 January 2020; Accepted 27 January 2020
Available online 31 January 2020

The conductive behavior of polymer composites is dependent on the loading and dispersion of conductive fillers in the matrix. For example, controlling the selective dispersion of conductive fillers at the interface or uniformly in a co-continuous phase could improve the conductivity efficiency of the fillers [20–22]. Choi et al. [17] prepared PBT/MWCNTs-*g*-PBT composites with higher conductivity and mechanical properties than PBT/MWCNTs composites, which is related to a better dispersion of MWCNTs and stronger interfacial adhesion between the MWCNTs and the PBT matrix by grafting PBT onto the carbon nanotubes. Wen et al. [23] found that graphite nanoplatelets (GNPs) in PBT/polycarbonate (PC) blends preferred to stay in the co-continuous PBT phase due to thermodynamic reasons. As a result, the conductivity of the ternary PBT/PC/GNPs composites with 3 vol% GNPs increased by 8 orders of magnitude compared with PBT/GNPs or PC/GNPs binary composites.

Although both toughness and conductivity of PBT can be improved, the routes to simultaneously enhance its toughness and conductivity have not been well reported. Li et al. [16] made PBT/PC composites with improved toughness and conductivity by adding elastomers and CNTs, whereas the CNTs exhibited nonselective dispersion in both polymeric phases, consequently a large(r) loading of CNTs was required to form a conductive network. The primary objective of this work is to simultaneously enhance the toughness and the conductivity of PBT by the synergetic effect of epoxidized elastomer as a toughening modifier and epoxidized CNTs (e-CNTs) as selectively dispersed conductive fillers. The synergetic effect was better realized through PBT chain-extension/branching which varied the viscosity ratio of PBT-to-elastomer, and in turn led to a significant decrease in inter-elastomer-particle distance. In addition, following the environmental protection and sustainable development strategies, recycled PBT was used as a raw material in this study. Therefore, this work provides a sustainable route, as schematically shown in Fig. 1, to make super-tough and antistatic PBT composites that can be (re-)used in automotive and electrical applications.

2. Experimentsexperiments

2.1. Materials

Recycled poly(butylene terephthalate) (PBT) with a melt flow rate of 27 g/10min (250 °C, 2.16 kg) and a melting temperature of 223 °C was received from Dongguan Zhangmutou Co., Ltd. Epoxy-groups containing elastomer, i.e., ethylene-vinyl acetate-glycidyl methacrylate copolymer (EVMG) containing 0.022 mol epoxy groups per 100 g and a vinyl acetate content of 60 wt%, is supplied by Arlanxeo (GER) GmbH. Styrene-acrylic-glycidyl methacrylate oligomers as rheology modifier (Joncryl®ADR4370) was provided by BASF. Hydroxyl multi-walled carbon nanotubes (h-CNTs) with a hydroxyl content of 1.0%, an average diameter of 8 nm and a length of 10–30 μm were purchased from Beijing Dekedao Gold Technology Co., Ltd. A silane coupling agent (γ-(2,3-epoxypropoxy) propyltrimethoxysilane, KH560, 98%) was obtained from Sinopharm Group Co., Ltd.

Fig. 1. Schematic diagram of recycling, functionalization and reuse of PBT materials.

2.2. Sample preparation

Synthesis of epoxidized CNTs (e-CNTs). Epoxidized CNTs (e-CNTs) were prepared by grafting KH560 onto the surface of h-CNTs [24], as illustrated in supporting information (Fig. S1). First, a KH560 solution (0.05 g/mL) with deionized water (10 mL) and ethanol (180 mL) was prepared. After adjusting the pH of the solution to be 4.0 with dilute hydrochloric acid, it was maintained at 40 °C for 2 h to complete the hydrolysis of -Si(O(CH_3))$_3$ of KH560. At the same time, the h-CNTs suspension in ethanol (0.04 g/mL) was prepared by ultrasound treatment. Subsequently, the h-CNTs suspension was added to KH560 solution and the mixture was stirred at 70 °C for 16 h to make sure the complete coupling reaction between the h-CNTs and the KH560. The e-CNTs, i.e., CNTs-*g*-KH560 nanohybrids, were finally obtained after purification with ethanol by 3 times to remove the unreacted KH560.

Preparation of PBT composites. After complete drying of the starting materials, PBT/EVMG/e-CNTs/ADR composites were prepared using the following procedures: 1) PBT and e-CNTs were first blended for 3 min in a Polylab-OS mixer (Haake, Germany) to create a grafting reaction between the PBT and the e-CNTs; 2) Subsequently, EVMG was added with an additional 3 min mixing to generate a reaction between the PBT and the EVMG; 3) ADR was finally fed into the Haake mixer followed by another 3 min mixing to achieve PBT chain extension/branching. The above-mentioned process is concisely monitored by the torque variation of PBT composite during blending, as shown in Fig. 2. The prepared PBT/EVMG/e-CNTs/ADR composites were denoted as PEC_xA_y, wherein P, E, C and A represent PBT, EVMG, e-CNTs and ADR, respectively, while x and y represent the weight percentage of e-CNTs and ADR in the composites, respectively. The mass ratio of PBT to EVMG was fixed at 80/20. All composites were prepared at 235 °C with a rotor speed of 60 rpm, including PBT/EVMG composite (P/E) for comparison. After compounding, specimens were prepared by compression molding at 240 °C for further characterization.

2.3. Characterization

Fourier transform infrared (FT-IR). The h-CNTs and e-CNTs were analyzed by FT-IR spectrometer (Nicolet 6700, Thermo Fisher Scientific,

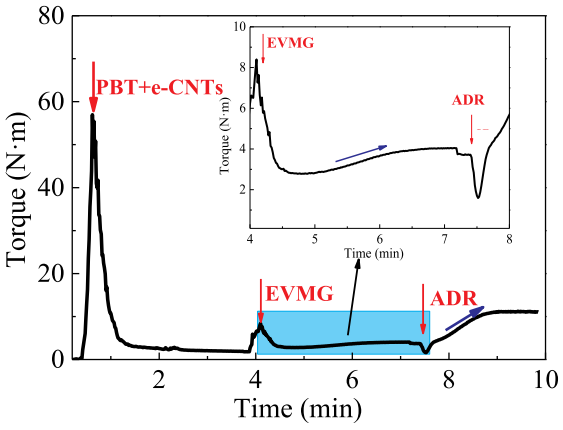

Fig. 2. The torque values of PBT-based composites (taking PEC_1A_1 as an example) as a function of time during preparation process. The red arrows indicate the addition of corresponding components. (For interpretation of the references to colour in this figure legend, the reader is referred to the Web version of this article.)

US) in attenuated total reflection (ATR) mode. The final spectrum of each sample was an average of 32 scans at a resolution of 4 cm^{-1} in the wavenumber range of 400–4000 cm^{-1}.

Thermogravimetric analysis (TGA). The decomposition behavior of CNTs before and after epoxidation was detected by a TGA instrument (1100SF, MettlerToledo, Switzerland) from 50 to 600 °C at 10 °C/min in a nitrogen atmosphere.

X-ray photoelectron spectroscopy (XPS). The XPS data of h-CNTs and e-CNTs were carried out with an electron spectrometer (Axis supra, Kratos, England) using monochromatized Al Ka radiation (hv = 1486.6eV, 225 W) as X-ray source.

Rheological behavior. The dynamic rheological behavior of PBT-based composites were investigated by a DHR-2 rheometer (TA, USA) at 240 °C with a constant strain of 3% in a frequency-sweep mode (from 100 to 0.01 Hz). The strain of 3% was pre-determined from a strain-sweep experiment to make the measurements in a linear viscoelastic strain range.

Mechanical properties. The tensile properties of the PBT-based composites were measured using a tensile tester (Instron 5967, USA) and the notched Izod impact tests were carried out according to ISO 180 using an impact tester on the standard sized rectangular bars at room temperature. Five measurements of each sample were tested to present the averaged values.

Scanning electron microscopy (SEM). The cross-sections of PBT-based composites after fracture in a liquid nitrogen environment and etching away the EVMG phase with xylene was observed by SEM (S-4800, HITACHI, Japan). The impact sections of samples were characterized by the same SEM. All the samples were sputtered with gold before observation.

Transmission electron microscopy (TEM). The micro phase-distribution of PBT-based composites was observed on a TEM instrument (JEM-2100plus, Japan) at an accelerating voltage of 200 kV. The specimens were microtomed to an ultrathin section (~80 nm thick) at −120 °C.

Electrical conductivity measurement. Electrical conductivity of PBT-based composites was tested on a digital high-resistance instrument (PC68, China). The samples with a diameter of 100 mm and a thickness of 0.5 mm were prepared through compression-molding processing at 240 °C and 10 MPa. Measurements of each sample repeated five times to obtain the average value.

3. Results and discussion

3.1. Characterization of e-CNTs

CNTs-*g*-KH560 nanohybrids (e-CNTs) were prepared by grafting epoxy-silane (KH560) on to hydroxyl CNTs (h-CNTs). FT-IR, TGA and XPS were used to characterize the chemical structures of the e-CNTs, as shown in Fig. 3. Compared with h-CNTs, the FT-IR spectra of e-CNTs in Fig. 3a/3b show new stretching vibration peaks corresponding to Si–O bond (1100 cm^{-1}) and C–H bond (2945 cm^{-1} and 2840 cm^{-1}), respectively [25]. KH560 contains Si–O and –CH_2– groups while CNTs do not. Therefore, the new stretching vibration peaks of e-CNTs confirmed that the KH560 was grafted onto the surface of CNTs.

The modification of CNTs by KH560 is further evidenced by the appearance of a silicon element on the surface of e-CNTs nanohybrids as detected via X-ray photoelectron spectra, i.e., only peaks of C1s and O1s are detected for h-CNTs, whereas typical Si 2p and Si 2s peaks [26] at around 102 eV and 153 eV appear in the XPS spectra of e-CNTs (Fig. 3c). Furthermore, the quantitative characterization of the grafting of KH560

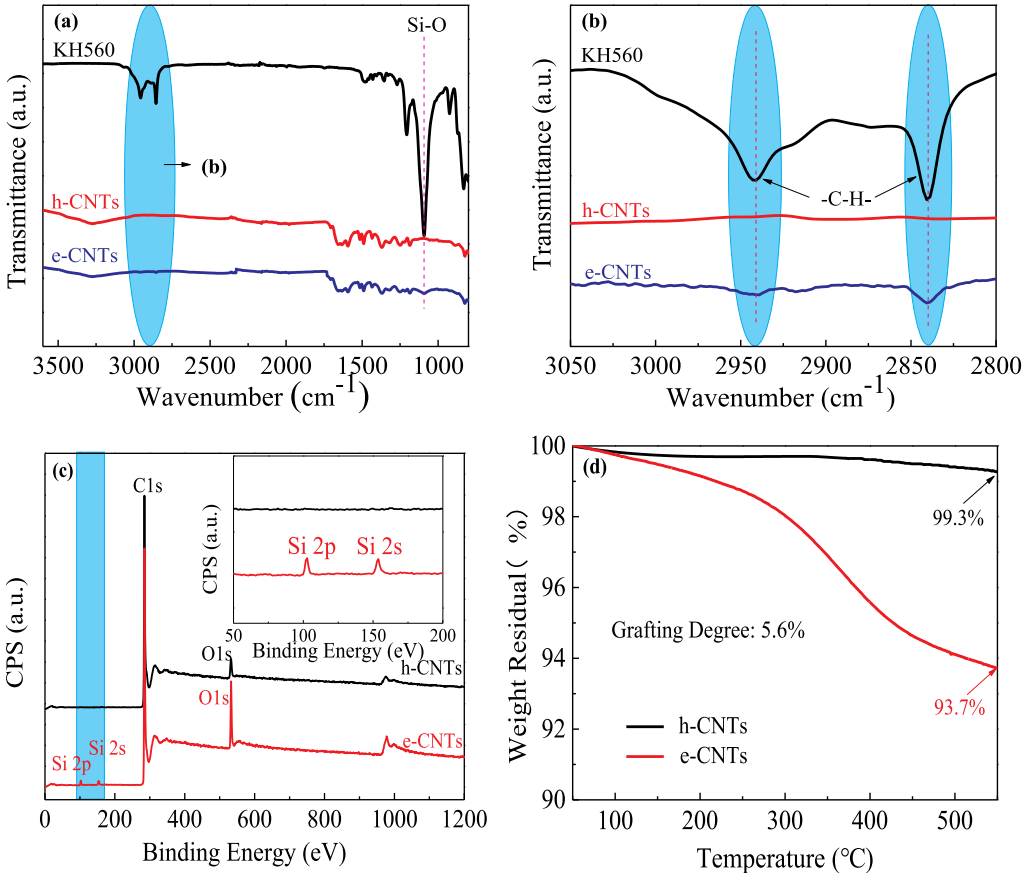

Fig. 3. (a), (b) FT-IR spectra of h-CNTs, e-CNTs and KH560, (c) XPS spectra and (d) TGA curves of h-CNTs and e-CNTs. The CPS (i.e. counts per second) in XPS spectra represents the relative intensity of photoelectron flow.

was also performed by TGA, and the curves were shown in Fig. 3d. It can be seen from the TGA curves that h-CNTs exhibit unobvious weight loss (<1 wt%) until 550 °C, in contrast with an apparent weight loss (6.3 wt %) in the case of e-CNTs nanohybrids. The extra weight loss is regarded as the thermal degradation of grafted KH560. Therefore, the grafted amount of the reacted KH560 was roughly calculated to be 5.6 wt% through the differences in final weight residuals [27].

3.2. Rheological behavior of PBT-based composites influenced by multi-reactions

In this study, multi-reactions between the terminal carboxyl/hydroxyl groups of PBT and the epoxy groups of other components (EVMG, ADR and e-CNTs) could occur in situ during the sample preparation process, as illustrated in Fig. 4.

The reaction between e-CNTs and PBT is confirmed by the appearance of carbonyl stretching vibration peak in FT-IR spectra of e-CNTs/PBT blends after removing unreacted PBT, as shown in Fig. S2. Such a reaction is purposely designed to facilitate the selective dispersion of e-CNTs in the PBT phase only, see discussion latter. The reactions between EVMG (or ADR) and PBT are confirmed by the torque changes of the rheometer after addition of EVMG and ADR, as shown in Fig. 2. The increase in torque indicates an increase in viscosity of the PBT phase due to PBT branching/coupling/crosslinking in the presence of EVMG and ADR, because only PBT is reactive with the epoxy groups of the rubbery EVMG and the ADR oligomers.

It can be inferred from the dominate structures proposed in Fig. 4 after each reaction that all these reactions play an important role in making long-branched chains and even partially cross-linked network structures. To better understand the microstructural evolution of PBT with these reactions, the dynamic rheological behaviors of the PBT-based composites were investigated to show the storage modulus (G′) and complex viscosity (η) as a function of frequency (Fig. 5).

It is shown clearly that the PBT-based composites exhibit a higher storage modulus and complex viscosity in the used frequency zone compared with neat PBT. Neat PBT exhibits a more Newtonian-like behavior at low frequency region as shown in Fig. 5. However, the melt viscosity (η) and storage modulus (G′) of PBT increase significantly after incorporation of EVMG and the P/E composite exhibits a shear-thinning behavior, indicating enhanced melt elasticity. This variation in rheology is related to the long-branched chain structure with longer relaxation time resulting from the reaction between PBT and EVMG, as shown in Fig. 4. In the presence of 1 wt% e-CNTs, the PEC_1 composite shows similar rheological behavior as the P/E composite, indicating that the low content of e-CNTs with small amount of epoxy groups could not significantly modify the chemical structure of PBT. However, both η and G′ increased strongly after the addition of ADR into the PEC_1, as shown in Fig. 5. This is attributed to the growth of PBT molecular chains with larger molecular weight after chain extension [28]. And additionally, the PEC_1A_1 composite exhibits a more obvious shear-thinning behavior and shows a platform at the low frequency region, i.e., indicative of the presence of network structures in this system [29,30]. The network structure here contains a continuous network, either physical (entanglements) or chemical (partially chemical crosslinks of long-branched PBT chains) and a dispersed network structure formed by overlapping e-CNTs, which is to be discussed in detail later. By the way, the increase of viscosity by chain extension has an acceptable effect on processing properties of composites in the higher shear regime. Thus, the reactions between PBT and other components (EVMG, e-CNTs, ADR) introduced both long-branched chains and cross-linked network into PECA composites as proven by the rheological experiments.

3.3. Morphology evolution of PBT-based composites

The melt-rheological behavior of the PBT-based composites was influenced more significantly by chain extension according to the discussion above. Consequently, SEM was used to examine the morphology evolution of the composites as a function of ADR content, as shown in Fig. 6.

In Fig. 6, EVMG is dispersed as spherical particles in the PBT matrix

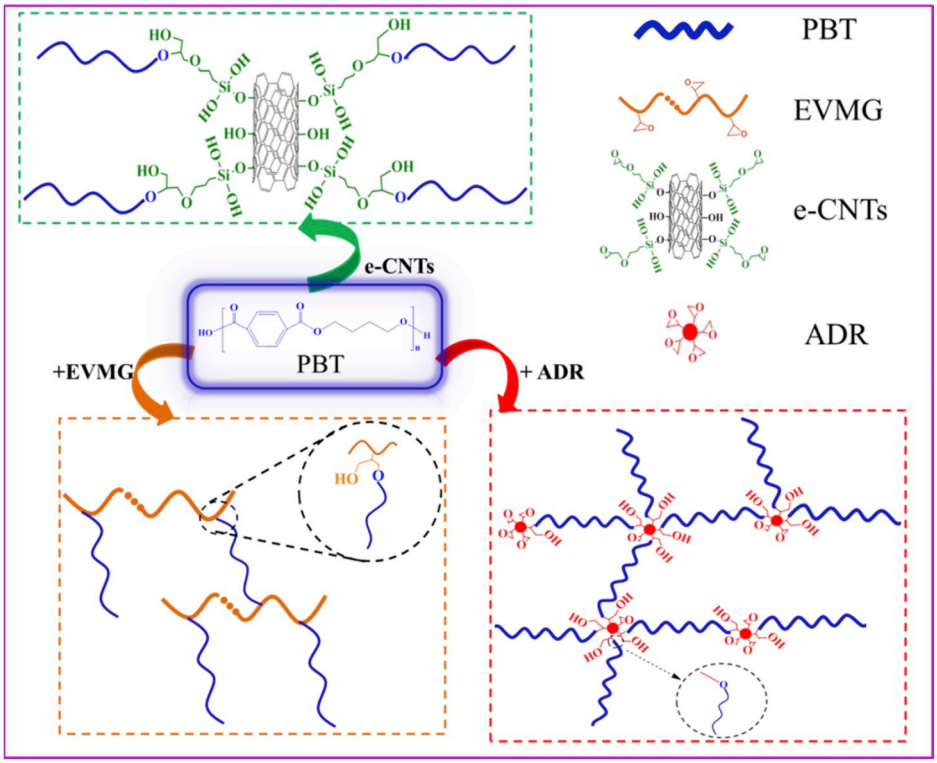

Fig. 4. Schematic diagrams of chemical reactions between the PBT and other components during processing.

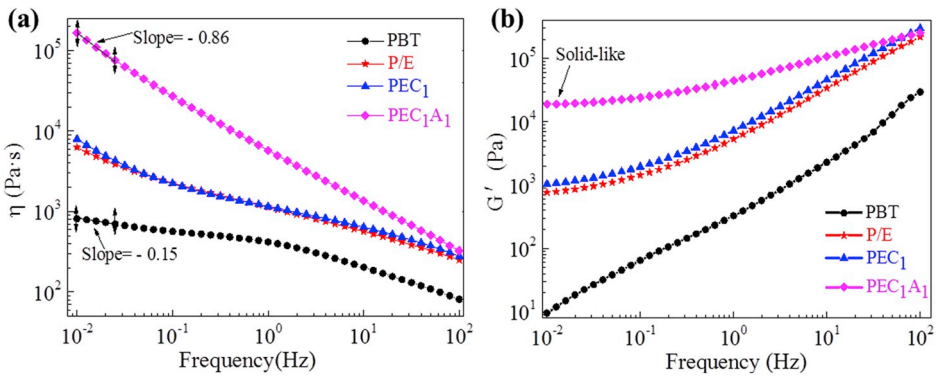

Fig. 5. (a) Complex viscosity and (b) storage modulus of the PBT-based composites as a function of scanning frequency.

in all composites. An obvious decrease in number-averaged particles size ($\overline{D}_n$) from 0.40 μm to 0.16 μm was observed with increasing the ADR content from 0 up to 1.0 wt%, as shown in Fig. 6. The higher ADR content is, the smaller the EVMG particles are. It is well-known in the physics of polymer blending that the $\overline{D}_n$ in polymer blends is related to the viscosity ratio of both matrix (η_m) and the dispersed phase (η_d), the interfacial tension (r) and the shear rate ($\dot{\gamma}$), as correlated below:

$$\overline{D}_n = \frac{Kr(\eta_d)^n}{(\eta_m)^{1-n}\dot{\gamma}} \quad (1)$$

Where, the constants K and n depend on the volume fraction of the dispersed phase (ϕ_d). It is reported that K = 4.0 and n = 0.84 for rubber/polyester blends at ϕ_d= 0.15 [31]. It can be understood that the reduction in EVMG particle size is mainly attributed to the change in viscosity ratio of PBT to EVMG since ADR could solely react with PBT leading to higher viscosity of PBT matrix. This remark is confirmed by the increase in processing torque (Fig. 2) and complex viscosity (Fig. 5a) of PECA composites after addition of ADR. Consequently, a greater shear force would be applied to the EVMG domains leading to a smaller size and denser dispersion. According to the rheology data in Fig. 5a and equation (1), the viscosity of PBT matrix with ARD is more sensitive to shear rate, and thus smaller $\overline{D}_n$ are expected at lower shear rates as well. Moreover, even a local interconnection of EVMG particles in the PECA compounds is observed at the ADR content of 1 wt% due to the considerable decrease of inter-particle distance, as shown more clearly in Fig. S3. Such evolution in morphology can be beneficial to the mechanical and conductivity properties of the PECA composites.

3.4. Mechanical properties of PBT-based composites

The mechanical properties of PBT and PBT-based composites with different ADR contents were studied by tensile and notched impact tests, as shown in Fig. 7.

The tensile strength of neat PBT is 45 MPa, which was reduced to 26 MPa after addition of the 20 wt% EVMG and 1 wt% e-CNTs. However, the tensile strength of the PEC_1A_x composites was regained up to 34 MPa with 1 wt% ADR (Fig. 7a) because of the extension/branching of PBT chains. On the other hand, the toughness of neat PBT was improved dramatically by incorporation of EVMG, i.e., the notched impact strength increased from 4 kJ/m^2 to 65 kJ/m^2 (Fig. 7b). Moreover, the notched impact strength of the PEC_1A_x composites was further enhanced to 88 kJ/m^2 and the elongation at break was increased from 150% to >310% after addition of 1.0 wt% ADR (Fig. 7c). The toughening mechanism is discussed below. To summarize, super-toughed PBT composites with good tensile strength can be obtained applying a chain extension/branching concept.

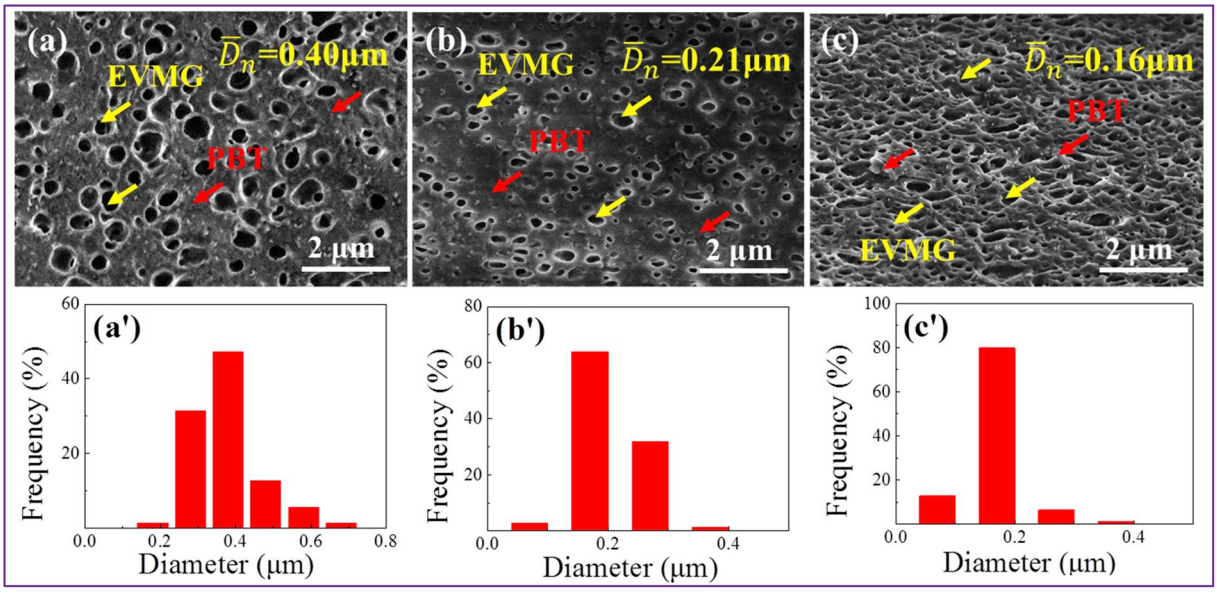

Fig. 6. SEM images (a/b/c) of the PEC_1A_x composites and the diameter distribution EVMG phase (a'/b'/c') as a function of ADR content: (a/a') 0 wt%, (b/b') 0.5 wt % and (c/c') 1.0 wt%. The red and yellow arrows indicate the PBT phase and cavities left by the EVMG phase after selective dissolution (see experimental section), respectively. (For interpretation of the references to colour in this figure legend, the reader is referred to the Web version of this article.)

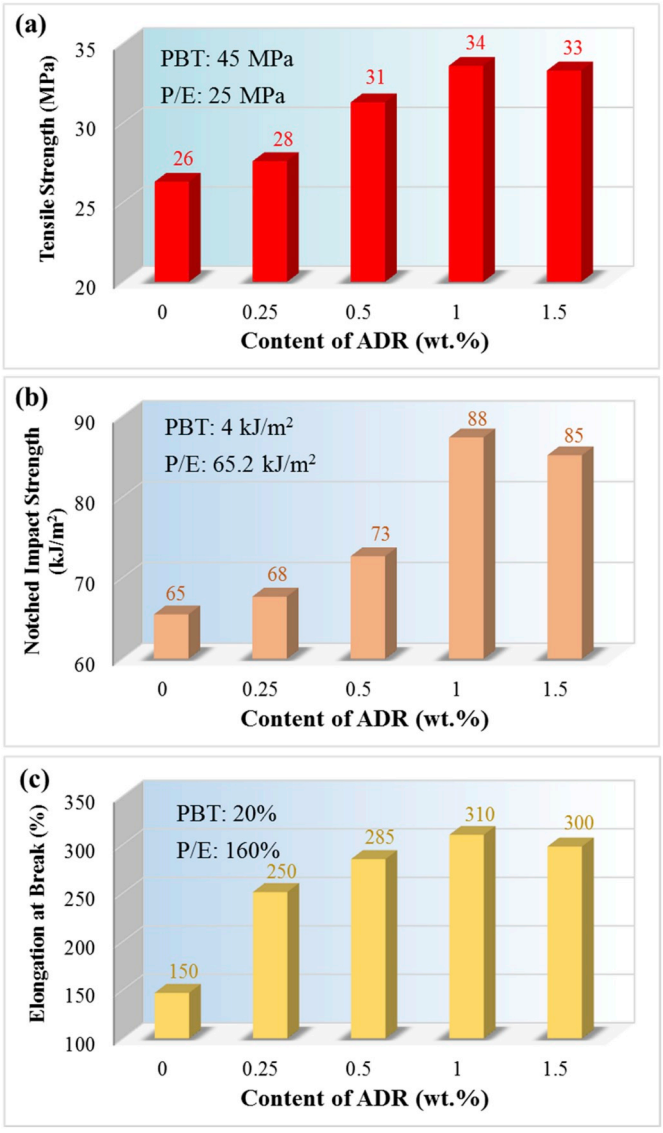

Fig. 7. (a) the tensile strength, (b) notched impact strength, (c) elongation at break of PEC_1A_x composites with different ADR contents. The error bar for the tensile strength, notched impact strength, and elongation at break are within 2 MPa, 4 kJ/m^2 and 15%, respectively.

3.5. Toughening mechanism analysis

In order to understand the toughening mechanism of PBT in the presence of EVMG and chain extension/branching, the impact-fractured surfaces of corresponding composites were studied using SEM, as shown in Fig. 8. PBT shows smooth surface after impact fracture (Fig. 8a), whereas both PEC_1A_0 and PEC_1A_1 exhibit significant band-like plastic deformation on the fractured surface which is mainly responsible for the improved toughness (Fig. 8b/c).

The special band-like patterns, taking the PEC_1A_0 composite as an example, are explained by the novel distribution of EVMG particles in the PBT matrix, as illustrated in Fig. 8d. The EVMG particles are overall uniformly dispersed in the PBT matrix (inset of Fig. 8d), but locally aggregated because PBT chains that grafted with EVMG could bond the adjacent EVMG particles together forming self-assembled EVMG-rich domains (yellow mark in Fig. 8d) and PBT-rich domains (blue mark in Fig. 8d). During the impact test experiment, the EVMG domains could absorb the impact energy by generating large deformation to terminate the shear bands of neighboring PBT-rich domains, and subsequently as

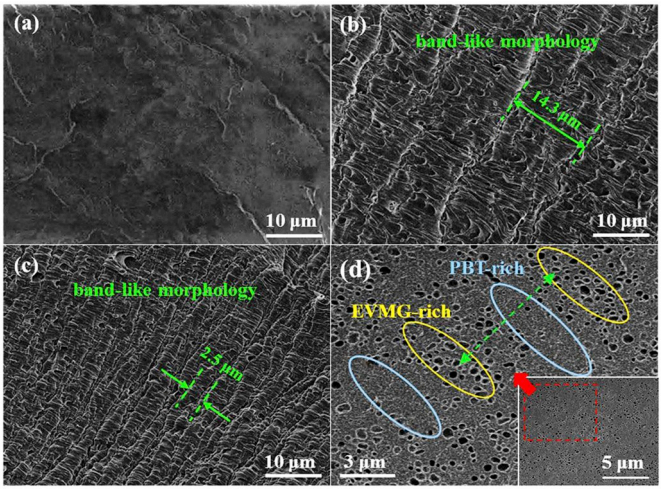

Fig. 8. SEM images of impact fractured surfaces of (a) PBT, (b) PEC_1A_0 and (c) PEC_1A_1 composites. (d) SEM images of cryo-fractured surface of PEC_1A_0 composite after etching away EVMG, while the inset image at right bottom of Fig. 8d is from the same sample but with larger area showing overall homogeneous morphology.

stress concentrator initiate new shear bands. These processes repeat continuously to dissipate impact energy entirely. Thus, the novel band-like stripes are resulted from sequential deformation of the alternate PBT-rich and EVMG-rich domains along the impact directions, leading to super toughness of the PECA composites.

It is worth noting that the width between band-shaped stripes become much smaller after chain extension/branching (green marks in Fig. 8b/c). This is well related to the reduced inter-particle distance (τ) of EVMG, which can be calculated by formula below assuming EVMG particles as spheres [32,33], i.e.,

$$\tau = \overline{D}_n \left[\left(\frac{\pi}{\phi_d} \right)^{1/3} - 1 \right] \tag{2}$$

Wherein the $\overline{D}_n$ and ϕ_d have the same physical meanings as formula 1. According to calculation, the inter-particle distance of EVMG is reduced from 910 nm to 360 nm after chain extension. Since smaller inter-particle distance facilitates superposition of stress fields around the EVMG particles, the band-like plastic deformation can penetrate the entire PBT matrix greatly improving the toughness of the PECA composites.

This argument is further proved by etching away the EVMG phase from the impact fractured surfaces, as shown in Fig. 9. Clearly, two phenomena could be observed, i.e., i) the cavities left by the EVMG domains in Fig. 9b' are much smaller than those in Fig. 9a', which is consistent with above morphology discussion (Fig. 6); ii) the cavities are dominantly located at the boundary of the band-like stripes that supports the above "propagation-termination-repropagation" hypothesis. Since the inter-particle distance of EVMG is significantly reduced after chain extension, the shear bonds encounter the EVMG-rich domains with a shorter distance, resulting in narrower and denser band-like morphology of the PEC_1A_1 than that of the PEC_1A_0 composite.

3.6. Conductive behavior of PBT-based composites

The electrical conductivity of the PECA composites was investigated as a function of e-CNTs content and the results are shown in Fig. 10a.

It is known that CNTs are ideal functional fillers to impart conductive and/or antistatic performance to polymeric materials [34,35]. As expected, the electrical conductivity of both $PECA_0$ and $PECA_1$ composites increased with increasing the content of e-CNTs (Fig. 10a). However, it is interesting to observe that the electrical conductivity of $PECA_1$ is

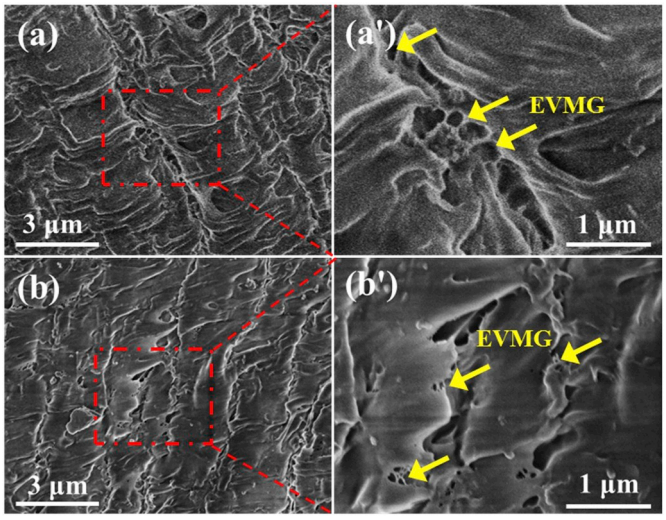

Fig. 9. SEM images of impact fracture surfaces of samples after etching EVMG away: (a/a') PEC_1A_0 and (b/b') PEC_1A_1. The yellow arrows indicate the cavities left by EVMG phase. (For interpretation of the references to colour in this figure legend, the reader is referred to the Web version of this article.)

higher than that of $PECA_0$ composites at the entire studied e-CNTs content range. Moreover, the conductivity of both $PECA_0$ and $PECA_1$ composites increases abruptly within a certain content range of e-CNTs, showing insulator-to-conductor transitions (ICT), and the ICT of $PECA_1$ composites occurs at lower e-CNTs content. The abrupt increase of electrical conductivity generally means a formation of conductive network [21,36]. The loading of conductive filler at the ICT point is called the percolation threshold. According to classical percolation theory [37], the conductivity of polymer composites is related to the concentration of conductive filler (ϕ) and the structure of the conductive network, namely:

$$\sigma = \sigma_0 (\phi\text{-}\phi_c)^t \quad (3)$$

Wherein the ϕ_c represents the percolation threshold of the system. σ_0 is a constant assigned to the plateau conductivity of completely loaded composites and the exponent t is used to predict the mechanism of network formation.

The percolation thresholds of the $PECA_0$ and $PECA_1$ composites calculated via equation (3) are inserted in Fig. 10a. Obviously, the percolation threshold of the PBT-based composite is reduced by 27% after chain extension by 1 wt% ADR. Although the percolation threshold is still higher than some reported values in other systems [34,38–40], this work provide an interesting route to form conductive networks at much lower filler loadings. To better visualize the evolution of e-CNTs network in the PECA composites, the rheological behaviors of PEC_xA_0 and PEC_xA_1 composites were investigated respectively as a function of e-CNTs contents, as shown in Fig. 11.

Rheological parameters such as storage modulus (G′) are very sensitive to a dispersion of filler in polymer composites [41], e.g., the formation of conductive network usually can be indicated by a platform in the G′ curves as a function of frequency [42]. As shown in Fig. 11, the G′ of both PEC_xA_0 and PEC_xA_1 composites increase with the e-CNTs content at low frequency regions and the G' ~ frequency curves gradually exhibit platforms, whereas, the platform of PEC_xA_1 composite appears at a lower content of e-CNTs (1.0 wt%). The slopes of G' ~ frequency curves at low frequency region are plotted in Fig. 10b with further fittings of starting and ending points of the e-CNTs networks as a function of e-CNTs content. The starting and ending points of PEC_xA_1 composites are 0.7 wt% and 1.1 wt%, respectively, which are 21% and 30% lower than those of PEC_xA_0 composites. Obviously, these rheological analyses are well consistent with the above conductivity results and theoretical calculations (Fig. 10a).

3.7. Chain extension assisted networking of e-CNTs

The mechanism of chain extension/branching brought by rheology modifiers assisting mechanical property improvement and CNTs network formation is shown in an artist view in Fig. 12.

After epoxidation of CNTs, the interfacial reaction between e-CNTs and PBT during the premixing process would lead to a chemical bonding between the CNTs and the PBT matrix. And thus, e-CNTs are selectively distributed in the PBT matrix, which is confirmed by the TEM images in Fig. 13. It means that the EVMG not only acts as a toughening modifier for PBT but also exhibits volume exclusion effect for e-CNTs. Since the inter-particle distance of EVMG is large in the $PECA_0$ composites (910 nm), the majority of CNTs has sufficient space forming coil-like structures (Figs. 12a and 13a). According to SEM and TEM observations (Figs. 6 and 13), the inter-particle distance of EVMG reduced from 910 to 360 nm after PBT chain extension/branching, consequently the CNTs are confined in the inter-particle areas in a more extended form (Figs. 12b and 13b). Thus, the e-CNTs are easier to interconnect with each other forming conductive networks at a lower percolation threshold. Furthermore, it remarked that the significant reduction in EVMG particle size and the finer dispersion of CNTs after PBT chain extension lead to both super toughness and high(er) tensile strength of the PBT-based composites. In summary, tough and antistatic PBT-based composites can be designed via a multistep reaction protocol using recycled resources.

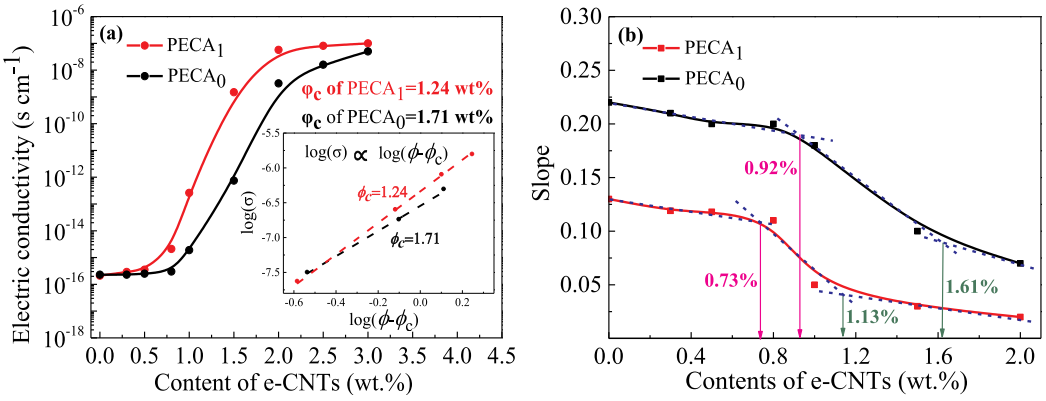

Fig. 10. (a) Electrical conductivity and (b) slope of storage modulus~frequency curves at low frequency regions of the PBT-based composites with different e-CNTs contents.

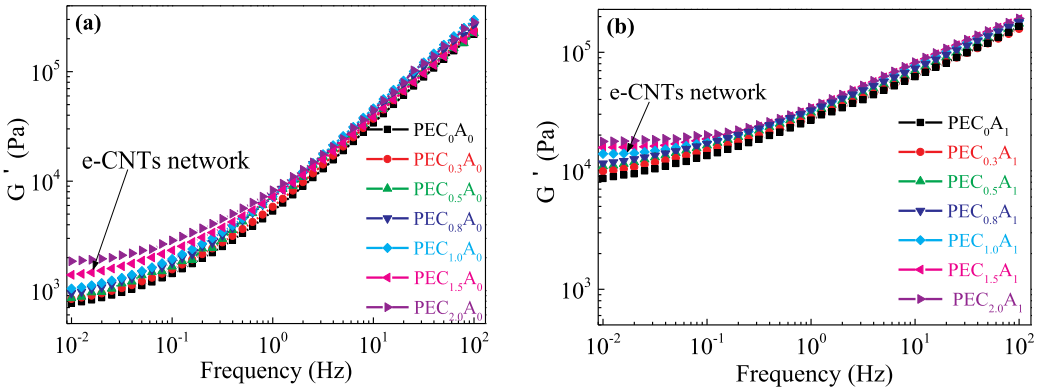

Fig. 11. Rheological behaviors of (a) $PECA_0$ and (b) $PECA_1$ composites with different e-CNTs contents.

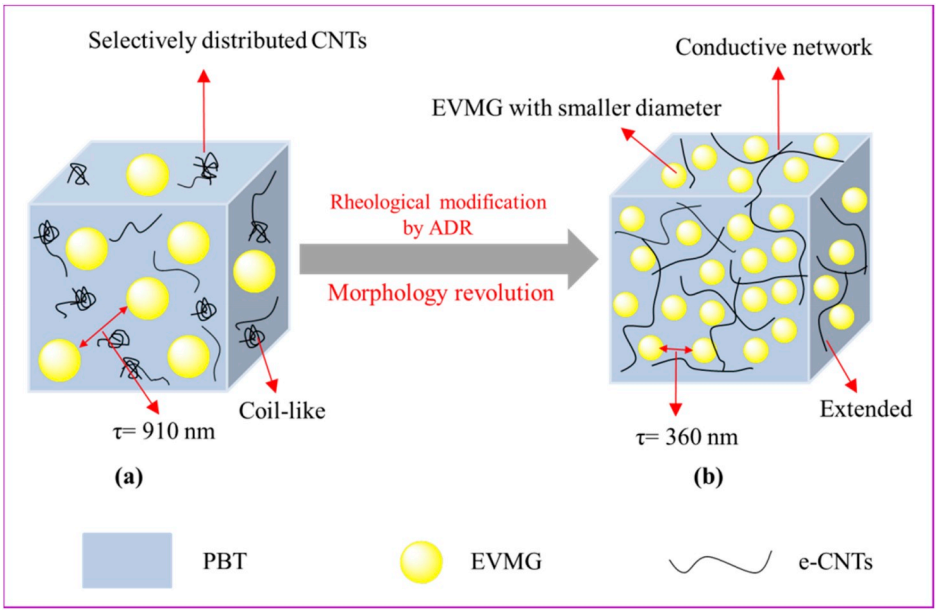

Fig. 12. Schematic diagram of the effect of chain extension/branching on PBT composite materials showing reduced particle size, inter-particle distance and favorable dispersion of CNTs.

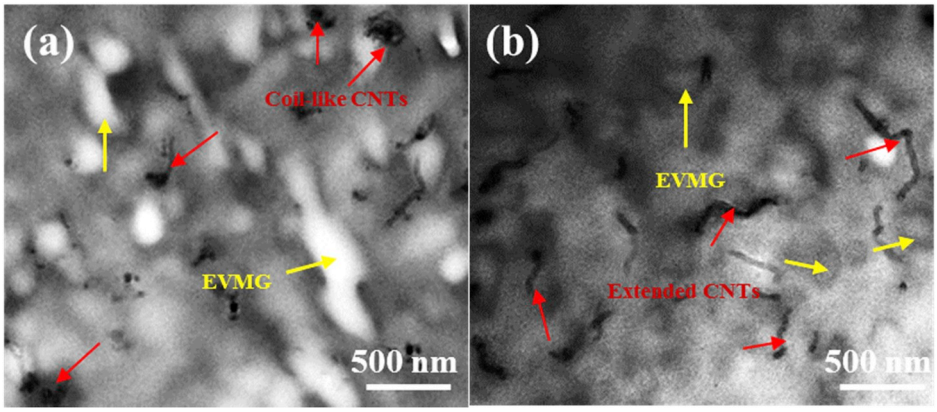

Fig. 13. TEM images of (a) PEC_1A_0 and (b) PEC_1A_1 composites with 1.0 wt% of e-CNTs. EVMG and e-CNTs have been marked by arrows for better visualization.

4. Conclusion

Highly modified composites, using recycled PBT as a matrix, were prepared by compounding with EVMG and a small quantity of e-CNTs and ADR. A continuous processing technique with multistep reactions was designed to achieve super toughness and antistatic PBT-based composites with low(er) CNTs loadings. Rheological measurements demonstrate that long-branched or even partially cross-linked structures

are formed in the composites after rheological modification of PBT, which eventually leads to smaller elastomer particle size and shorter inter-particle distance of the elastomer domains. On the one hand, the conductivity and rheological measurements confirmed that the conductive network of e-CNTs in the PBT phase is easier to form due to the volume exclusion effect of EVMG and further morphological optimization by ADR. On the other hand, the impact measurements demonstrate that EVMG and ADR exhibit synergistic toughening effect on the PBT materials. The toughening mechanism is related to the overall homogeneous dispersion of EVMG particles with smaller diameter and shorter inter-particle distance and the local interaction of EVMG particles. Therefore, this work not only provides an interesting route for super-tough and antistatic PBT-based composites but also opens an effective way to prepare high performance polymeric materials for automotive and electrical applications.

Declaration of competing interest

The authors declare that they have no known competing financial interests or personal relationships that could have appeared to influence the work reported in this paper.

CRediT authorship contribution statement

Ying Cao: Data curation, Investigation, Writing - original draft. **Pengwu Xu:** Validation, Formal analysis. **Baogou Wu:** Validation, Formal analysis. **Martin Hoch:** Writing - review & editing. **Pieter Jan Lemstra:** Writing - review & editing. **Weijun Yang:** Writing - review & editing. **Weifu Dong:** Writing - review & editing. **Mingliang Du:** Writing - review & editing. **Tianxi Liu:** Writing - review & editing. **Piming Ma:** Conceptualization, Supervision.

Acknowledgements

This work is supported by the National Natural Science Foundation of China (51873082), the Excellent Youth Natural Science Foundation of Jiangsu Province (BK20170053), and the MOE & SAFEA 111 Project (B13025). We would also like to acknowledge Dr. Roelof van der Meer (formerly BASF) and Dr. Theo Hoeks (SABIC Europe) for their valuable contributions.

Appendix A. Supplementary data

Supplementary data to this article can be found online at https://doi.org/10.1016/j.compscitech.2020.108043.

References

[1] J.H. Zhu, J.L. Cai, W.C. Xie, P.H. Chen, M. Gazzano, M. Scandola, R.A. Gross, Poly (butylene 2,5-furan dicarboxylate), a biobased alternative to PBT: synthesis, physical properties, and crystal structure, Macromolecules 46 (2013) 796–804, https://doi.org/10.1021/ma3023298.

[2] Y. Sasanuma, Y. Wagai, N. Suzuki, D. Abe, Conformational characteristics and configurational properties of poly (butylene terephthalate) and structure–property relationships of aromatic polyesters, Polymer 54 (2013) 3904–3913, https://doi.org/10.1016/j.polymer.2013.05.044.

[3] N. Fu, G.H. Li, Q.X. Zhang, N.Y. Wang, X.W. Qu, Preparation of a functionalized core–shell structured polymer by seeded emulsion polymerization and investigation on toughening poly (butylene terephthalate), RSC Adv. 4 (2014) 1067–1073, https://doi.org/10.1039/C3RA44163F.

[4] Y.P. Hao, W. Li, S.L. Sun, H.L. Zhang, G. Gao, L. Dong, Poly (butylene terephthalate) toughening with butadiene-epoxy-functionalized methyl methacrylate core–shell copolymer, J. Macromol. Sci. B 54 (2015) 1267–1281, https://doi.org/10.1080/00222348.2015.1079092.

[5] C.S. Wu, H.T. Liao, Preparation and characterization of functionalized graphite/poly(butylene terephthalate) composites, Polym. Bull. 72 (2015) 1799–1816, https://doi.org/10.1007/s00289-015-1372-x.

[6] W.Y. Su, K.S. Min, R.P. Quirk, In situ copolymerization and compatibilization of polyester and polystyrene blends. II. Thermally and chemically induced reaction and mechanical properties, Polymer 42 (2001) 5121–5134, https://doi.org/10.1016/s0032-3861(00)00777-1.

[7] C.C. Hu, S.S. Chang, N.Y. Liang, Preparation and characterization of carbon black/polybutylene terephthalate/polyethylene terephthalate antistatic fiber with sheath–core structure, J. Text. Inst. 107 (2016) 976–984, https://doi.org/10.1080/00405000.2015.1077022.

[8] H. Schmalz, V. Abetz, R. Lange, M. Soliman, New thermoplastic elastomers by incorporation of nonpolar soft segments in PBT-based copolyesters, Macromolecules 34 (2001) 795–800, https://doi.org/10.1021/ma001226p.

[9] C. Lavilla, E. Gubbels, A.M. Ilarduya, B.A.J. Noordover, C.E. Koning, S. Munoz-Guerra, Solid-state modification of PBT with cyclic acetalized galactitol and D-mannitol: influence of composition and chemical microstructure on thermal properties, Macromolecules 46 (2013) 4335–4345, https://doi.org/10.1021/ma400760d.

[10] X.W. Tang, W.H. Guo, G.R. Yin, B.Y. Li, C.F. Wu, Reactive extrusion of recycled poly(ethylene terephthalate) with polycarbonate by addition of chain extender, J. Appl. Polym. Sci. 104 (2007) 2602–2607, https://doi.org/10.1002/app.24410.

[11] X. Jin, N. Fu, H.L. Ding, N. Zhao, J.B. Sang, X.L. Li, S. Abbas, X.W. Xu, F.B. Meng, J. Li, Y. Fan, C.C. Tang, Effects of h-BN on the thermal and mechanical properties of PBT/PC/ABS blend based composites, RSC Adv. 5 (2015) 58171–58175, https://doi.org/10.1039/C5RA09746K.

[12] L. Tang, L.L. Wang, P.X. Chen, J.F. Fu, P. Xiao, N.B. Ye, M.Q. Zhang, Toughness of ABS/PBT blends: the relationship between composition, morphology, and fracture behavior, J. Appl. Polym. Sci. 135 (2018) 46051, https://doi.org/10.1002/app.46051.

[13] C. Meng, J.P. Qu, Mechanical and thermal properties of polybutylene terephthalate/ethylene-vinyl acetate blends using vane extruder, e-Polym. 18 (2018) 67–73, https://doi.org/10.1515/epoly-2017-0073.

[14] L. Yang, H. Chen, S.K. Jia, X. Lu, J.T. Huang, X.X. Yu, K.H. Ye, G.J. He, J.P. Qu, Influences of ethylene–butylacrylate–glycidyl methacrylate on morphology and mechanical properties of poly (butylene terephthalate)/polyolefin elastomer blends, J. Appl. Polym. Sci. 131 (2014), https://doi.org/10.1002/app.40660.

[15] A. Dorigato, M. Brugnara, A. Pegoretti, Synergistic effects of carbon black and carbon nanotubes on the electrical resistivity of poly (butylene–terephthalate) nanocomposites, Adv. Polym. Technol. 37 (2018) 1744–1754, https://doi.org/10.1002/adv.21833.

[16] J.L. Li, X.F. Wang, C.J. Yang, J.H. Yang, Y. Wang, J.H. Zhang, Toughening modification of polycarbonate/poly(butylene terephthalate) blends achieved by simultaneous addition of elastomer particles and carbon nanotubes, Composites, Part A-Appl. S. 90 (2016) 200–210, https://doi.org/10.1016/j.compositesa.2016.07.006.

[17] E.Y. Choi, S.W. Kim, C.K. Kim, In situ grafting of polybutylene terephthalate onto multi-walled carbon nanotubes by melt extrusion, and characteristics of their composites with polybutylene terephthalate, Compos. Sci. Technol. 132 (2016) 101–107, https://doi.org/10.1016/j.compscitech.2016.07.003.

[18] H.J. Zhou, H. Deng, L. Zhang, Q. Fu, Significant enhancement of thermal conductivity in polymer composite via constructing macroscopic segregated filler networks, ACS Appl. Mater. Interfaces 9 (2017) 29071–29081, https://doi.org/10.1021/acsami.7b07947.

[19] P.W. Xu, W.J. Yang, D.Y. Niu, M. Yu, M.L. Du, W.F. Dong, M.Q. Chen, P.J. Lemstra, P.M. Ma, Multifunctional and robust polyhydroxyalkanoate nanocomposites with superior gas barrier, heat resistant and inherent antibacterial performances, Chem. Eng. J. 122864 (2019), https://doi.org/10.1016/j.cej.2019.122864.

[20] J.R. Huang, C. Mao, Y.T. Zhu, W. Jiang, X.D. Yang, Control of carbon nanotubes at the interface of a co-continuous immiscible polymer blend to fabricate conductive composites with ultralow percolation thresholds, Carbon 73 (2014) 267–274, https://doi.org/10.1016/j.carbon.2014.02.063.

[21] P.M. Ma, P. Lv, P.W. Xu, M.L. Du, H. Zhu, W.F. Dong, M.Q. Chen, Design of bio-based conductive and fast crystallizing nanocomposites with controllable distribution of multiwalled carbon nanotubes via interfacial stereocomplexation, Chem. Eng. J. 336 (2018) 223–232, https://doi.org/10.1016/j.cej.2017.11.092.

[22] A.C. Baudouin, J. Devaux, C. Bailly, Localization of carbon nanotubes at the interface in blends of polyamide and ethylene–acrylate copolymer, Polymer 51 (2010) 1341–1354, https://doi.org/10.1016/j.polymer.2010.01.050.

[23] B.Y. Wen, X.L. Zheng, Effect of the selective distribution of graphite nanoplatelets on the electrical and thermal conductivities of a polybutylene terephthalate/polycarbonate blend, Compos. Sci. Technol. 174 (2019) 68–75, https://doi.org/10.1016/j.compscitech.2019.02.017.

[24] X.W. Zhao, H.T. Wang, Z.A. Fu, Y.J. Li, Enhanced Interfacial Adhesion by Reactive Carbon Nanotubes: new route to high-performance immiscible polymer blend nanocomposites with simultaneously enhanced toughness, tensile strength, and electrical conductivity, ACS Appl. Mater. Interfaces 10 (2018) 8411–8416, https://doi.org/10.1021/acsami.8b01704.

[25] H. Guo, J. Liu, Q. Wang, M.L. Liu, C.Y. Du, B.A. Li, L.F. Feng, High thermal conductive poly(vinylidene fluoride)-based composites with well-dispersed carbon nanotubes/graphene three-dimensional network structure via reduced interfacial thermal resistance, Compos. Sci. Technol. 181 (2019) 107713, https://doi.org/10.1016/j.compscitech.2019.107713.

[26] J.C. Gu, P. Xiao, P. Chen, L. Zhang, H.L. Wang, L.W. Dai, L.P. Song, Y.J. Huang, J. W. Zhang, T. Chen, Functionalization of biodegradable PLA nonwoven fabric as superoleophilic and superhydrophobic material for efficient oil absorption and oil/water separation, ACS Appl. Mater. Interfaces 9 (2017) 5968–5973, https://doi.org/10.1021/acsami.6b13547.

[27] K.W. Lee, J.W. Chung, S.Y. Kwak, Flexible Poly(vinyl chloride) nanocomposites reinforced with hyperbranched polyglycerol-functionalized graphene oxide for enhanced gas barrier performance, ACS Appl. Mater. Interfaces 9 (2017) 33149–33158, https://doi.org/10.1021/acsami.7b10257.

[28] J. Liu, L. Ye, X.W. Zhao, Preparation of long–chain branched poly (ethylene terephthalate): molecular entanglement structure and toughening mechanism, Polym. Eng. Sci. 59 (2019) 1190–1198, https://doi.org/10.1002/pen.25099.
[29] E.V. Hemelrijck, P.V. Puyvelde, S. Velankar, C.W. Macosko, P. Moldenaers, Interfacial elasticity and coalescence suppression in compatibilized polymer blends, J. Rheol. 48 (2004) 143–158, https://doi.org/10.1122/1.1634987.
[30] H.D. Huang, J.Z. Xu, Y. Fan, L. Xu, Z.M. Li, Poly(L-lactic acid) crystallization in a confined space containing graphene oxide nanosheets, J. Phys. Chem. B 117 (2013) 10641–10651, https://doi.org/10.1021/jp4055796.
[31] S.H. Wu, Formation of dispersed phase in incompatible polymer blends: interfacial and rheological effects, Polym. Eng. Sci. 27 (1987) 335–343, https://doi.org/10.1002/pen.760270506.
[32] S.H. Wu, Phase structure and adhesion in polymer blends: a criterion for rubber toughening, Polymer 26 (1985) 1855–1863, https://doi.org/10.1016/0032-3861(85)90015-1.
[33] Z.H. Liu, X.D. Zhang, X.G. Zhu, Z.N. Qi, F.S. Wang, Effect of morphology on the brittle ductile transition of polymer blends.1. A new equation for correlating morphological parameters, Polymer 38 (1997) 5267–5273, https://doi.org/10.1016/s0032-3861(97)00075-x.
[34] G. Wang, L. Wang, L.H. Mark, V. Shaayegan, G. Wang, H. Li, G. Zhao, C.B. Park, Ultralow-threshold and lightweight biodegradable porous PLA/MWCNT with segregated conductive networks for high-performance thermal insulation and electromagnetic interference shielding applications, ACS Appl. Mater. Interfaces 10 (2017) 1195–1203, https://doi.org/10.1021/acsami.7b14111.
[35] X. Gao, A.I. Isayev, X.P. Zhang, J. Zhong, Influence of processing parameters during ultrasound assisted extrusion on the properties of polycarbonate/carbon nanotubes composites, Compos. Sci. Technol. 144 (2017) 125–138, https://doi.org/10.1016/j.compscitech.2017.03.019.
[36] K. Cheah, M. Forsyth, G.P. Simon, Processing and morphological development of carbon black filled conducting blends using a binary host of poly (styrene co-acrylonitrile) and poly (styrene), J. Polym. Sci., Part B: Polym. Phys. 38 (2000) 3106–3119, https://doi.org/10.1002/1099-0488(20001201)38:23<3106::aid-polb120>3.0.co;2-2.
[37] D. Staufler, A. Aharony, Introduction to Percolation Theory, Taylor and Franis, London, 1992.
[38] Y.Y. Shi, J.H. Yang, T. Huang, N. Zhang, C. Chen, Y. Wang, Selective localization of carbon nanotubes at the interface of poly (L-lactide)/ethylene-co-vinyl acetate resulting in lowered electrical resistivity, Compos. B Eng. 55 (2013) 463–469, https://doi.org/10.1016/j.compositesb.2013.07.012.
[39] R. Dou, Y. Shao, S.L. Li, B. Yin, M.B. Yang, Structuring tri-continuous structure multiphase composites with ultralow conductive percolation threshold and excellent electromagnetic shielding effectiveness using simple melt mixing, Polymer 83 (2016) 34–39, https://doi.org/10.1016/j.polymer.2015.12.005.
[40] J. Chen, X. Liao, W. Xiao, J.M. Yang, Q.Y. Jiang, G.X. Li, Facile and green method to structure ultralow-threshold and lightweight polystyrene/MWCNT composites with segregated conductive networks for efficient electromagnetic interference shielding, ACS Sustain. Chem. Eng. 7 (2019) 9904–9915, https://doi.org/10.1021/acssuschemeng.9b00678.
[41] D.H. Xu, Z.G. Wang, Role of multi-wall carbon nanotube network in composites to crystallization of isotactic polypropylene matrix, Polymer 49 (2008) 330–338, https://doi.org/10.1016/j.polymer.2007.11.041.
[42] C.M. Huang, H.W. Bai, H. Xiu, Q. Zhang, Q. Fu, Matrix crystallization induced simultaneous enhancement of electrical conductivity and mechanical performance in poly (l-lactide)/multiwalled carbon nanotubes (PLLA/MWCNTs) nanocomposites, Compos. Sci. Technol. 102 (2014) 20–27, https://doi.org/10.1016/j.compscitech.2014.07.016.